Investigation of gain enhancement of electrically small antennas using double-negative, single-negative, and double-positive materials

B. Ghosh,* S. Ghosh,† and A. B. Kakade‡
Department of Electronics and Electrical Communication Engineering, Indian Institute of Technology, Kharagpur, West Bengal, 721 302, India
(Received 5 March 2008; published 26 August 2008)

In this paper, it is shown that a double-negative or a mu-negative shell can be used to achieve a very high gain for an electrically small loop. It is also seen that together with the high gain, the metamaterial shell can be used to achieve a very uniform gain characteristic with respect to the shell dimensions. This is accomplished by a proper choice of the media parameters of the metamaterial shell and the region surrounding the antenna. This significantly eases the fabrication constraints and the close tolerances on the shell which was a major drawback towards the practical realization of the shell. Also, significant power gain can be obtained when the radiated power from the metamaterial shell is compared to the power radiated by a loop of the same radius as the outer radius of the shell. In addition, it is also found that a double-positive shell of the same dimensions as the metamaterial shell can be used to significantly increase the gain of the infinitesimal antenna. The power gain characteristics show distinct resonant peaks in this case. Excellent matching characteristics are observed corresponding to the radiated power gain.

DOI: 10.1103/PhysRevE.78.026611 PACS number(s): 41.20.Jb

I. INTRODUCTION

Long after Veselago investigated wave propagation in metamaterials in 1967 [1], intense research endeavors are being recently focused on these materials [2–5]. Metamaterials are characterized by oppositely directed phase and group velocities. Since the electric field vector, the magnetic field vector and the wave vector of the electromagnetic wave in these media form a left-handed triad, these are also referred to as left-handed materials. These are also known as double-negative (DNG) materials as the permittivity and permeability of these materials are simultaneously negative. In contrast, single negative (SNG) media refer to those materials with either one of the permittivity or permeability values positive and the other negative. Materials with permittivity negative and permeability positive are called epsilon-negative (ENG) while those with permeability negative and permittivity positive are called mu-negative (MNG) materials. It has been shown that the phase delay in a double-positive (DPS) medium can be compensated by a corresponding phase advance in a DNG medium leading to the potential development of extremely miniaturized antennas and resonant structures [6,7].

In the present work, gain enhancement and characterization of electrically small antennas surrounded by metamaterial and DPS shells is addressed. Electrically small antennas and antenna efficiency have been studied by several researchers in the past [8–29]. Interaction of antennas with a dielectric shell cover has been addressed in [30–34]. The principal motivation for the current work is the basic proposition reported in [35–45] regarding the behavior of electrically small dipoles in free space and DNG media. It was originally shown in [35,36] that significant gain enhancement of an electrically small dipole can be accomplished by surrounding it with a DNG shell. An electrically small dipole in free space is a very poor radiator due to its large capacitive impedance [10–24]. However, it was observed by Ziolkowski and Kipple in [35] that the infinitesimal dipole can be made resonant by enclosing the antenna with a DNG medium, as the capacitive and inductive impedances offered by the DPS and DNG media can cancel each other out. A similar configuration for an infinitesimal dipole surrounded by an ENG shell in [40] was shown to demonstrate a very large power gain, due to the resonance between the inductive load offered by the ENG shell and the capacitive impedance of the dipole in the inner medium. Practical realization of the ENG material using a lumped-element and meander-line based implementation was addressed in [41]. A multilayer spherical configuration was presented in [42–45] to achieve gain enhancement for an electrically small antenna. Gain enhancement of an electric line source by concentric metamaterial cylindrical shells was proposed in [46,47]. Design topologies for performance enhancement of planar and nonplanar electrically small antennas was addressed in [48–52]. These include designs based on the coupling between a driven inductive antenna element with a self-resonant capacitive structure.

However, it was emphasized in [35] that in spite of the very large and promising gain characteristics obtained with the metamaterial shell, the biggest difficulty in practically realizing the metamaterial shell was the extremely narrow tolerance value and the small thickness of the DNG shell. This topic is addressed in this work. In this paper, it is first shown that DNG/SNG media can also be used to enhance the radiated power for an electrically small loop. In addition, it is seen that the permittivities and permeabilities of the DNG/SNG media can be chosen so as to offer a large and uniform gain characteristic over a wide range of shell thickness, thus increasing the mechanical tolerance and the shell thickness

*bghosh@ece.iitkgp.ernet.in
†susmita.gh@gmail.com
‡kakadeanand@yahoo.com

considerably for either the electrically small loop or the dipole. Very good reactance ratios are obtained over the uniform gain region making the reactive power very small compared to the radiated power. The radiated power gain of the DNG/MNG shell was also compared with respect to a loop antenna of the same radius as the outer radius of the shell and reasonably good power gains were obtained.

In addition, the gain enhancement characteristics of the antenna using a DPS shell is also studied. It is shown that a DPS shell, which is easy to fabricate and do not possess dispersion, can also be used to considerably enhance the radiated power gain of the electrically small antenna. To the best of our knowledge, gain enhancement of infinitesimal antennas using DPS shells has not been reported. It might be noted here that gain enhancement of electrically small antennas has been demonstrated using an ENG shell in [40,42] with an in-depth analysis of the interaction of the electrically small antenna and the shell. However, the conclusion that gain enhancement is not possible with DPS shells is different from the conclusion reached in this paper. The power gain characteristics of the electrically small loop surrounded by the DPS shell is compared to the power gain profile obtained using the metamaterial shell. The source free resonant frequencies for the TE_{nmp} modes of the two-layer dielectric resonator antenna (DRA), obtained recently through the Green's function analysis of the N-layer DRA, is seen to exactly match the resonant peaks of the power gain for the electrically small loop surrounded by the DPS shell.

II. RADIATION CHARACTERISTICS OF ELECTRICAL LOOP IN DPS AND DNG MEDIA

Let us consider an infinitesimally small loop of radius a surrounded by a DPS medium. The electric and magnetic fields radiated by the loop are given by [23]

$$E_\phi = \frac{\eta(ka)^2 I_0 \sin\theta}{4r}\left(1+\frac{1}{jkr}\right)e^{-jkr}, \tag{1}$$

$$H_\theta = \frac{-(ka)^2 I_0 \sin\theta}{4r}\left(1+\frac{1}{jkr}-\frac{1}{(kr)^2}\right)e^{-jkr}, \tag{2}$$

$$H_r = \frac{jka^2 I_0 \cos\theta}{2r^2}\left(1+\frac{1}{jkr}\right)e^{-jkr}, \tag{3}$$

$$E_r = E_\theta = H_\phi = 0. \tag{4}$$

The complex power crossing a closed spherical surface around a loop is given by

$$P = \frac{1}{2}\oiint_S (\vec{E}\times\vec{H}^*)\cdot\hat{n}dS = P_{\text{rad}} + jP_{\text{reac}}, \tag{5}$$

where $\hat{n}$ is unit vector normal to the closed surface.

Using (1)–(4) in (5), the complex power radiated by the infinitesimal circular loop surrounded by unbounded DPS medium can be obtained as [23]

$$P_{\text{DPS}} = \eta\left(\frac{\pi}{12}\right)(ka)^4|I_0|^2\left(1+j\frac{1}{(kr)^3}\right). \tag{6}$$

From (6), the average power radiated by the loop is given by

$$P_{\text{rad}}^{\text{DPS}} = \eta\left(\frac{\pi}{12}\right)(ka)^4|I_0|^2. \tag{7}$$

From (7), it can be observed that an electrically small loop, like a small electric dipole [35,23] is not a good radiator as the radiated power decreases as the quadratic power of the electrical radius of the loop. Further, the normalized reactance for the loop at $r=a$, defined as in the dipole case in [35,23], is given by

$$X_R(a) = \frac{P_{\text{reac}}}{P_{\text{rad}}} = \frac{X_{\text{ant}}}{R_{\text{rad}}}. \tag{8}$$

Using (5), (6), and (8), normalized reactance parameter for the loop can be obtained as

$$X_R^{\text{DPS}}(a) = \frac{1}{(ka)^3}. \tag{9}$$

It can be observed from (9) that an electrically small loop possesses a large inductive reactance, and therefore is not useful as a radiator. It has been noted that a similar phenomenon occurs for the electrically small dipole case. However, it was shown in [35] that a DNG shell can be effectively utilized to enhance the radiated power manifold for electrically small dipoles. This is due to the fact that the power radiated by a small dipole in a DPS medium possesses a large capacitive reactance while correspondingly, the reactive power is highly inductive in a DNG medium. Thus, the reactive part of the power of an infinitesimal dipole in a DPS medium can be tuned out by surrounding the dipole by a DNG shell. The radiated power in the case of the loop in a DNG medium is investigated to examine if the same effect can be obtained in the loop case. As the propagation constant k changes sign in a DNG medium, the radiated power of the loop in the DNG medium becomes

$$P_{\text{DNG}} = \eta\left(\frac{\pi}{12}\right)(ka)^4|I_0|^2\left(1-j\frac{1}{(kr)^3}\right) = P_{\text{DPS}}^*. \tag{10}$$

From (10) and (6), it can be seen that the imaginary component of radiated power changes sign when the loop is immersed in a DNG medium. This can be used to enhance the radiated power for the loop in a DPS medium by using a DNG shell, similar to the power enhancement in the dipole case. In this case, the power gain occurs due to compensation of the large inductive load seen by the small loop in a DPS medium by a corresponding capacitive load offered by the DNG medium, resulting in a conjugate match situation as $P_{\text{DNG}}=P_{\text{DPS}}^*$. This conclusion is important as the electric loop in the x-y plane is equivalent to a z-directed slot, which from the above can be matched to free space using a DNG medium, for slots of electrically small dimensions. Thus, efficient and miniaturized slot radiators can be constructed using this technique and one is no longer constrained to the slot dimensions to achieve resonance.

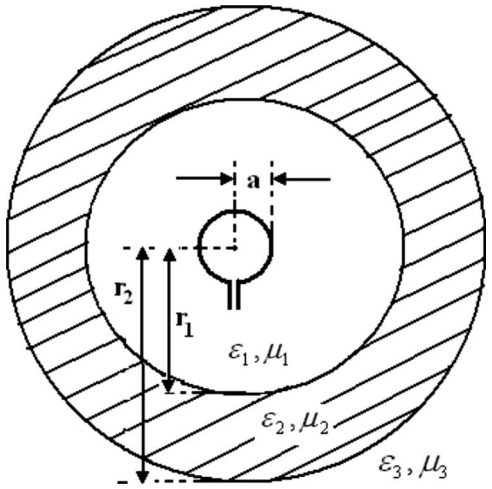

FIG. 1. Electrically small loop surrounded by a dielectric shell.

III. ANALYSIS OF AN INFINITESIMAL LOOP SURROUNDED BY THE DNG SHELL

Figure 1 shows an infinitesimal electric loop of radius a centered inside a DPS sphere (region 1). The sphere is surrounded by a DNG shell (region 2) of inner and outer radii r_1 and r_2, respectively. Region 3 being free space, extends from r_2 to ∞. A time-harmonic dependence $e^{j\omega t}$ is assumed and suppressed throughout. The electric and magnetic fields in this structure are obtained as follows.

Region 1. We have

$$E_\phi^1 = \frac{\eta_1 (k_1 a)^2 I \sin\theta}{4r}\left(1 + \frac{1}{jk_1 r}\right)e^{-jk_1 r} - C_1 \sin\theta j_1(k_1 r), \tag{11}$$

$$H_\theta^1 = \frac{-(k_1 a)^2 I \sin\theta}{4r}\left(1 + \frac{1}{jk_1 r} - \frac{1}{(k_1 r)^2}\right)e^{-jk_1 r} - \frac{C_1 \sin\theta j_1(k_1 r)}{j\omega\mu_1 r}[k_1 r j_1'(k_1 r) + j_1(k_1 r)], \tag{12}$$

$$H_r^1 = \frac{j(k_1 a)^2 I \cos\theta}{2r^2}\left(1 + \frac{1}{jk_1 r}\right)e^{-jk_1 r} + \frac{2C_1 \cos\theta}{j\omega\mu_1 r} j_1(k_1 r), \tag{13}$$

$$E_r^1 = E_\theta^1 = H_\phi^1 = 0. \tag{14}$$

Region 2. We have

$$E_\phi^2 = -C_2 \sin\theta[j_1(k_2 r) + C_3 n_1(k_2 r)], \tag{15}$$

$$H_\theta^2 = \frac{-C_2 \sin\theta}{j\omega\mu_2 r}\{k_2 r[j_1'(k_2 r) + C_3 n_1'(k_2 r)] + [j_1(k_2 r) + C_3 n_1(k_2 r)]\}, \tag{16}$$

$$H_r^2 = \frac{2C_2 \cos\theta}{j\omega\mu_2 r}[j_1(k_2 r) + C_3 n_1(k_2 r)], \tag{17}$$

$$E_r^2 = E_\theta^2 = H_\phi^2 = 0. \tag{18}$$

Region 3. We have

$$E_\phi^3 = -C_4 \sin\theta h_1^{(2)}(k_3 r), \tag{19}$$

$$H_\theta^3 = \frac{-C_4 \sin\theta}{j\omega\mu_3 r}[(k_3 r) h_1^{(2)'}(k_3 r) + h_1^{(2)}(k_3 r)], \tag{20}$$

$$H_r^3 = \frac{2C_4 \cos\theta}{j\omega\mu_3 r} h_1^{(2)}(k_3 r), \tag{21}$$

$$E_r^3 = E_\theta^3 = H_\phi^3 = 0, \tag{22}$$

where $j_1(kr)$ and $n_1(kr)$ represent the first-order spherical Bessel functions of the first and second kind, respectively, and $h_1^{(2)}(kr)$ represents the first-order spherical Hankel function of the second kind [53]. The prime in the above equations represents the derivative with respect to function's argument. The unknown constants $C_1 - C_4$ are found by applying the continuity of E_ϕ and H_θ at radii r_1 and r_2 and are given by

$$C_1 = \frac{X_3 X_4 + j\omega\mu_2 X_2}{-\frac{\mu_2}{\mu_1}[(k_1 r_1) j_1'(k_1 r_1) + j_1(k_1 r_1)] + X_4 j_1(k_1 r_1)}, \tag{23}$$

$$C_2 = \frac{C_1 j_1(k_1 r_1) - X_3}{j_1(k_2 r_1) + C_3 n_1(k_2 r_1)}, \tag{24}$$

$$C_3 = \frac{-(k_2 r_2) j_1'(k_2 r_2) + (X_1 - 1) j_1(k_2 r_2)}{(k_2 r_2) n_1'(k_2 r_2) - (X_1 - 1) n_1(k_2 r_2)}, \tag{25}$$

$$C_4 = \frac{C_2[j_1(k_2 r_2) + C_3 n_1(k_2 r_2)]}{h_1^{(2)}(k_3 r_2)}, \tag{26}$$

where

$$X_1 = \frac{\mu_2}{\mu_3}\left(1 + \frac{(k_3 r_2) h_1^{(2)'}(k_3 r_2)}{h_1^{(2)}(k_3 r_2)}\right), \tag{27}$$

$$X_2 = \frac{(k_1 a)^2 I_0}{4}\left(1 + \frac{1}{jk_1 r_1} - \frac{1}{(k_1 r_1)^2}\right)e^{-jk_1 r_1}, \tag{28}$$

$$X_3 = \frac{\eta_1 (k_1 a)^2 I_0}{4r_1}\left(1 + \frac{1}{jk_1 r_1}\right)e^{-jk_1 r_1}, \tag{29}$$

$$X_4 = 1 + \frac{(k_2 r_1) j_1'(k_2 r_1) + C_3 n_1'(k_2 r_1)}{j_1(k_2 r_1) + C_3 n_1(k_2 r_1)}. \tag{30}$$

IV. NUMERICAL RESULTS

A. DPS-DNG/SNG-free space

In this section, the formulation in Sec. III is used to compute the power gain obtained using a DNG shell surrounding

the electrically small loop. All results in this paper were obtained based on our MATLAB code. Verification using commercially available simulation tools like the high-frequency structure Simulator (HFSS) or computation of input impedance was not possible due to lack of access to the considerably high computational resource needed for the simulation of electrically small antenna structures [40].

The loop is placed in a spherical region (region 1) with permittivity ε_0 and permeability μ_0, as shown in Fig. 1. As in [35], the media parameters for the DNG shell (region 2) were initially chosen to be $(\varepsilon_2, \mu_2)=(-\varepsilon_0, -\mu_0)$. Region 3 is free space with the same parameters as region 1. The excitation frequency of the loop is 10 GHz with the loop radius $a=\lambda_0/1000=30$ μm, a loop current of 1 A and the radius of the inner shell $r_1=\lambda_0/300=100$ μm, in accordance with [35], in order to compare the results with the electrically small dipole case. The power gain of the loop was computed as

$$P_{\text{gain}} = \frac{P_{\text{rad,DNG}}}{P_{\text{rad,DPS}}}. \tag{31}$$

It was seen that exactly the same power gain characteristics versus the outer shell radius r_2 was obtained for the electrically small loop as for the infinitesimal dipole in Ref. [35]. All other features of the power gain behavior including the reactance ratio characteristics for the dipole, are found to be exactly similar for the loop case, and are not repeated for brevity. With reference to Fig. 3 and Fig. 4 in [35], it should however be noted that the field profiles in the case of the loop are interchanged with respect to the dipole due to duality. The variation in the real part of E_ϕ with distance from the loop is identical to that of the variation in the imaginary part of H_ϕ with distance from the dipole and vice versa for the imaginary E_ϕ for the loop and the real H_ϕ for the dipole. Correspondingly, the real and/or imaginary part of H_θ varies with distance from the loop in exactly the same manner as the imaginary and/or real part of E_θ, respectively, with distance from the dipole.

Next, the influence of the material parameters of the different layers on the power gain characteristics is examined. It was shown earlier [Ref. [35], Figs. 11(a) and 11(b)] that for an outer shell radius of $r_2=185.8004$ μm of the DNG medium surrounding a small dipole, a very high gain of 92.18 dB could be realized by choosing the material parameters for region 2 to be $\varepsilon_{r2}=\mu_{r2}=-3$. For these same material parameters and dimensions, an identical gain characteristic is obtained for the infinitesimal loop. It was also noted that the resonance width is too narrow and the tolerance on r_2 very small, which was reported to be the most major difficulty in [35] towards a practical design. In addition, it was also reported in [35] that the DNG shell itself was very thin making the synthesis extremely difficult. It is shown in this paper that by a proper adjustment of material parameters of the medium surrounding the antenna and of that of the DNG shell, both these limitations can be overcome. Also, it was found that unlike the cases treated in [35–40,42], the permeability of the medium around the infinitesimal antenna (region 1) for the electrically small loop must be nonunity in order for the gain characteristics to be uniform with variation

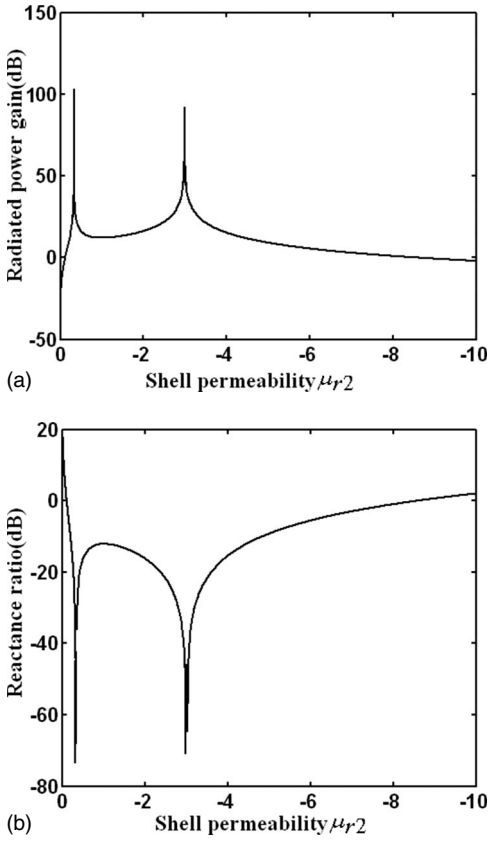

FIG. 2. (a) Radiated power gain and (b) reactance ratio versus μ_{r2} of an infinitesimal electric loop surrounded by a DNG shell, where $r_1=100$ μm, $r_2=185.8004$ μm, $a=30$ μm, $\varepsilon_{r1}=1$, $\mu_{r1}=1$, $\varepsilon_{r2}=-1$.

in the outer shell radius. Similarly, in order to obtain uniform gain characteristics with the electrically small dipole, the permittivity in region 1 should be nonunity. Thus, the choice of media parameters in region 1 and region 2 have a significant impact on the gain characteristics. The parametric variation of the individual media parameters to achieve optimally high and uniform power gain characteristics for the electrically small loop is discussed below.

In Fig. 2(a), the variation in gain with permeability of region 2 is shown for the electrically small loop, with the permittivity of region 2 fixed at $\varepsilon_{r2}=-1$. Two distinct gain peaks are visible in the figure for $\mu_{r2}=-0.3347$ and $\mu_{r2}=-2.99$. The gain was computed at the value of $r_2=185.8004$ μm corresponding to the peak of the power gain curve in Fig. 11(a) of [35]. Also, good reactance ratio characteristics are observed in Fig. 2(b) corresponding to the peak gains in Fig. 2(a). Figures 3(a) and 3(b) illustrate the variation in gain and reactance ratio with variable permittivity for the DNG shell ε_{r2} for a fixed $\mu_{r2}=-1$. It can be seen from Figs. 2 and 3 that the power gain is completely dependent on μ_{r2} and a change in ε_{r2} has no effect on the gain characteristics. A complementary behavior is observed in the dipole case where ε_{r2} affects the gain but μ_{r2} does not. This eases the constraint on design of the DNG shell as the power gain is decided by only one of the material parameters.

The change in the radiated power gain is next investigated with varying media parameters in the region surrounding the

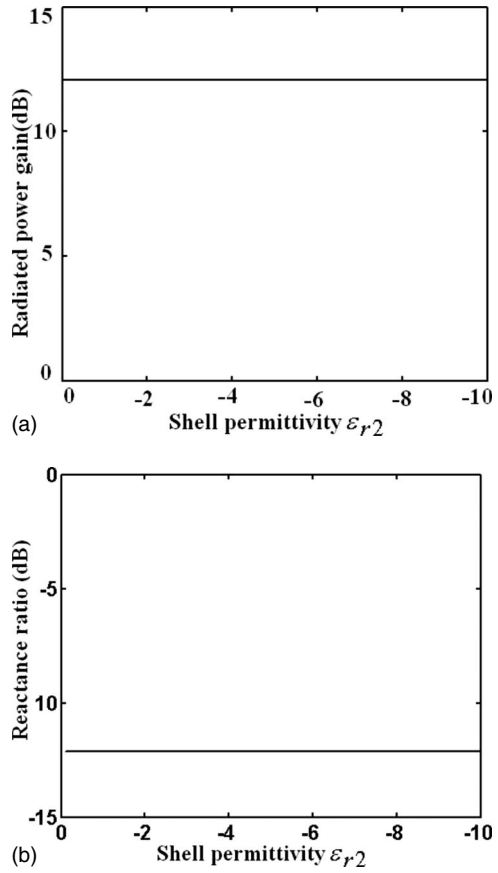

FIG. 3. (a) Radiated power gain and (b) reactance ratio versus ε_{r2} of an infinitesimal electric loop surrounded by a DNG shell, where $r_1=100$ μm, $r_2=185.8004$ μm, $a=30$ μm, $\varepsilon_{r1}=1$, $\mu_{r1}=1$, $\mu_{r2}=-1$.

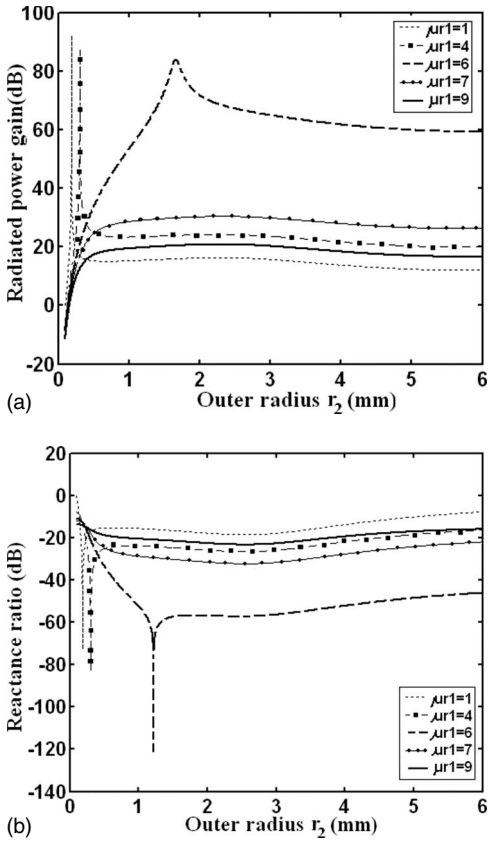

FIG. 4. (a) Radiated power gain and (b) reactance ratio of an infinitesimal electric loop surrounded by a DNG shell with different values of permeabilities in region 1 and variable outer radius r_2 with inner radius $r_1=100$ μm, $a=30$ μm, $\varepsilon_{r1}=1$, $\varepsilon_{r2}=-3$, $\mu_{r2}=-3$.

infinitesimal loop and that of the DNG shell. Figure 4(a) shows the power gain obtained by using media with different permeabilities in region 1. The curve corresponding to $\mu_{r1}=1$ is for the same case as treated in Fig. 11(a) of [35]. It can be observed from Fig. 4 that for $\mu_{r1}=6$, a high power gain above 60 dB is obtained over a large range of values of the outer shell radius r_2 from 1.18 mm to 5 mm. The gain peaks at 83.86 dB for $r_2=1.66$ mm. This implies that a large design tolerance can be obtained for the outer shell radius for $\mu_{r1}=6$ over which the gain characteristics are uniform. For $\mu_{r1}=1$ or 4, a very high power gain above 80 dB is obtained. However, the resonance behavior with respect to r_2 for these permeabilities is very sharp and as such realizing the design is more difficult, as noted before in [35]. Also, it is clear from Fig. 3(a) that for values of permittivity larger than $\mu_{r1}=6$, the power gain characteristics degrade. Despite this fact, from the gain characteristics for $\mu_{r1}=7$, a power gain of more than 20 dB can be achieved in this case over a wide range for $r_2 \geqslant 0.36$ mm.

Next, the effect of varying the permittivity of the DNG shell is studied [Fig. 5(a)], where the permeability of region 1 is maintained at the optimum value of $\mu_{r1}=6$. It is seen that gain characteristics are best for $\varepsilon_{r2}=-1$, where a stable power gain of more than 60 dB is obtained over 1.32 mm $\leqslant r_2 \leqslant 6$ mm. As can be observed from Fig. 5(a), the permittivity of the DNG shell has a prominent effect in improving the gain characteristics. From $\varepsilon_{r2}=-5$ to $\varepsilon_{r2}=-1$, the peak of the power gain curves shift to the right and a larger gain is obtained over a wider range of r_2. For example, compared to the improved gain characteristics using $\varepsilon_{r2}=-1$, a power gain of more than 60 dB is realizable for $\varepsilon_{r2}=-5$ over only 1.105 mm $\leqslant r_2 \leqslant 2.4$ mm. The gain peaks also get broader as the permittivity of the DNG shell becomes less negative. It is thus observed that the shell permittivity ε_{r2} has a significant impact in increasing the gain and bandwidth in Fig. 5(a) when the material surrounding the loop antenna possess a higher permeability than free space. Also, the peak gains are almost at the same level for different values of ε_{r2}. The gain peaks, however, occur at progressively larger values of r_2 as the permittivity of region 2 changes from a more to a less negative value. This yields flexibility to the designer, as, corresponding to a given DNG shell thickness, the permittivity of the shell can be appropriately chosen to achieve the power gain peak.

Figure 6(a) illustrates the effect of a variation in the permeability of the DNG shell, with the optimum values of $\mu_{r1}=6$, $\varepsilon_{r2}=-1$ chosen from above. It can be seen that a very good gain characteristic is obtained for $\mu_{r2}=-3$. The peak gain reaches 81.37 dB for an outer shell radius of $r_2=2.6$ mm. Also a very uniform gain profile is obtained over a large range of variation in r_2. This is the same curve as for the case $\varepsilon_{r2}=-1$ in Fig. 5(a). Due to the large design tolerance afforded by the geometry, the design is very easy to

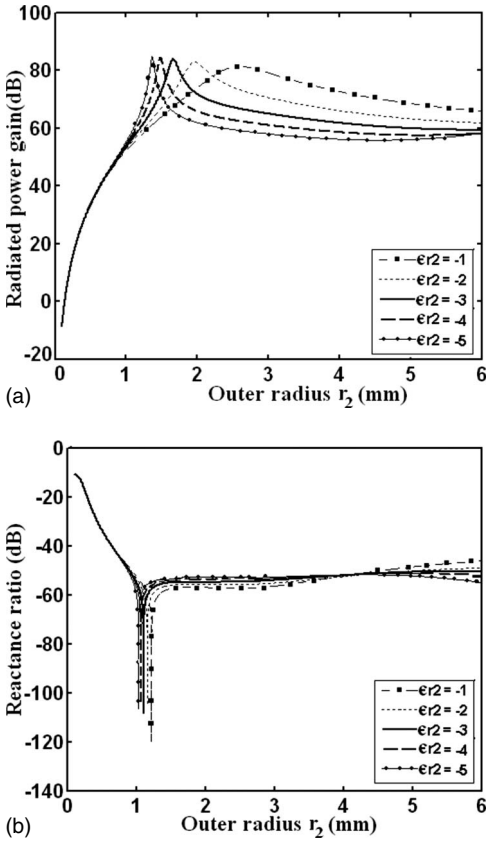

FIG. 5. (a) Radiated power gain and (b) reactance ratio of an infinitesimal electric loop surrounded by a DNG shell with different values of permittivities in region 2 and variable outer radius r_2 with inner radius $r_1=100$ μm, $a=30$ μm, $\varepsilon_{r1}=1$, $\mu_{r1}=6$, $\mu_{r2}=-3$.

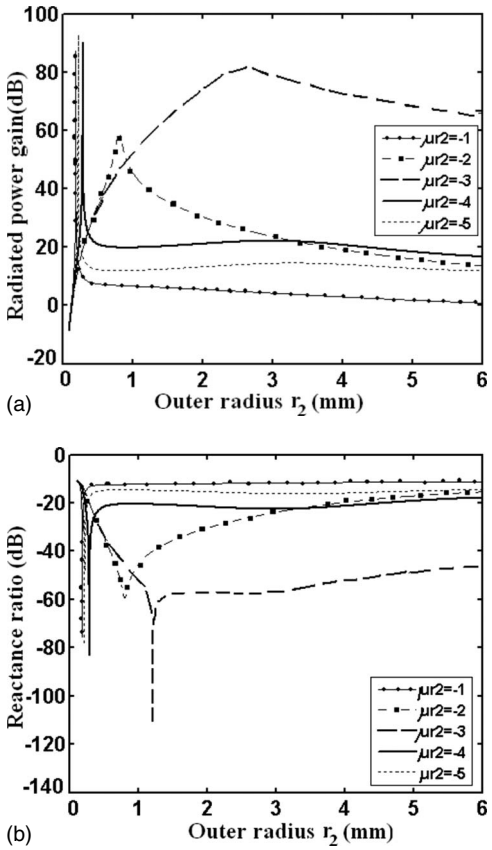

FIG. 6. (a) Radiated power gain and (b) reactance ratio of an infinitesimal electric loop surrounded by a DNG shell with different values of permeabilities in region 2 and variable outer radius r_2 with inner radius $r_1=100$ μm, $a=30$ μm, $\varepsilon_{r1}=1$, $\mu_{r1}=6$, $\varepsilon_{r2}=-1$.

realize without compromising on the gain performance. For $\mu_{r2}=-2$ and -4, the gain is seen to be very stable and greater than 20 dB over a wide variation in r_2, with a peak gain of 59.33 dB at $r_2=0.81$ mm for $\mu_{r2}=-2$. However, the sharpness of resonance for $\mu_{r2}=-1$, -4, and -5 reduces the design tolerance near the peak power point. Also, for $\mu_{r2}\geqslant -1$ or $\leqslant -5$, the gain characteristics beyond the resonance degrade compared to the gain profile obtained with $\mu_{r2}=-2$, -3, and -4. The power gain versus r_2 for different values of ε_{r1} of the medium surrounding the loop antenna is shown in Fig. 7(a). The gain characteristic for $\varepsilon_{r1}=1$ in this case is the same as that for $\mu_{r2}=-3$ in Fig. 6(a), with a peak gain of 81.37 dB for $r_2=2.6$ mm. It might be noted that the gain characteristics have been shown up to an outer shell radius of 15 mm in Fig. 7(a). It can be thus seen from Fig. 7(a) that the design tolerance can be very significantly increased, as the DNG shell can be made much thicker. It can be observed that the DNG shell thickness is only 85.8004 μm at the power gain resonance using $\mu_{r1}=1$ in Fig. 11(a) of [35] with the other media parameters as $\varepsilon_{r1}=1$, $\varepsilon_{r2}=-3$, $\mu_{r2}=-3$. This is a very thin DNG shell which prevents its practical realization with current metamaterial synthesis techniques, as noted in that paper. Also, the range of r_2 over which the power gain can be achieved is very small [35]. However, it is seen that using a proper selection of media parameters in region 1 and region 2, a high and stable gain characteristic can be achieved over a large range of the outer shell radius. As the permittivity values increase over the free space value of $\varepsilon_{r1}=1$, the gain characteristic slowly degrade until $\varepsilon_{r1}=5$. However, a wide spatial range of r_2 with slowly varying power gain is obtained for all values of ε_{r1}. As a result, the design is relatively much less sensitive on both the variation in ε_{r1} and r_2. This fact is particularly important due to the fact that the electric loop in the horizontal plane has the same field profile of a z-directed slot. This slot can be viewed as the excitation source for the spherical resonator in region 1 loaded by the DNG shell. In this context, the permittivity of region 1 can be used to control the coupling to the slot and thus provides additional design flexibility without substantially affecting the gain. For a permittivity value of 5 in region 1, the power gain characteristics is better than the other cases for $r_2\geqslant 4.24$ mm, with a power gain of 71 dB at $r_2=4.24$ mm. In addition, the gain with $\varepsilon_{r1}=5$ is almost uniform with r_2 in this range, which further reduces the sensitivity to mechanical tolerance. Also, the thickness of the DNG shell is even more in this case, compared to that corresponding to the gain peak for $\varepsilon_{r1}=1$. It can thus be seen from Fig. 7 that uniform gain characteristics can be achieved over a large range of the outer shell radius of 2.6 mm. $\leqslant r_2 \leqslant 15$ mm. The power gain decreases for $\varepsilon_{r1}\geqslant 5$. From the above, it can be seen that using the parameter values $\varepsilon_{r1}=1$, $\mu_{r1}=6$, $\varepsilon_{r2}=-1$, $\mu_{r2}=-3$ for region 1 and region 2, an optimized design in terms of power gain and bandwidth can be

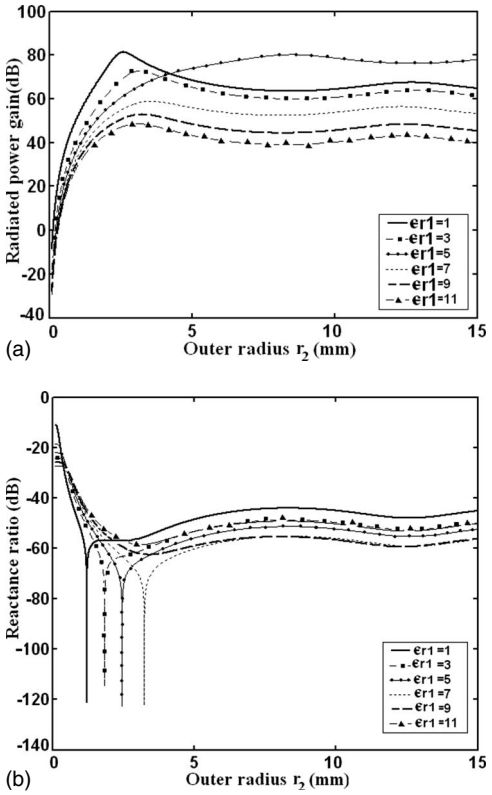

FIG. 7. (a) Radiated power gain and (b) reactance ratio of an infinitesimal electric loop surrounded by a DNG shell with different values of permittivities in region 1 and variable outer radius r_2 with inner radius $r_1=100$ μm, $a=30$ μm, $\mu_{r1}=6$, $\varepsilon_{r2}=-1$, $\mu_{r2}=-3$.

obtained for the outer shell radius $r_2<4.24$ mm. For larger values of r_2, a high and uniform gain characteristic can be obtained using the media parameters as $\varepsilon_{r1}=5$, $\mu_{r1}=6$, $\varepsilon_{r2}=-1$, $\mu_{r2}=-3$.

The reactance ratio corresponding to the case of Fig. 7(a) is shown in Fig. 7(b). It can be observed that though the power gain peaks in Fig. 7(a) do not exactly coincide with the reactance minima in Fig. 7(b), which has been also noted in [35], very good reactance ratios are obtained for all values of ε_{r1} corresponding to the entire uniform power gain regions in Fig. 7(a). This enables very good matching for the electrically small loop surrounded by the DNG shell. This, combined with the fact that the design tolerances are greatly enhanced, makes the topology ideal for achieving a very high gain from an infinitesimal antenna element over a very wide design margin and a thicker DNG shell which makes fabrication very easy. The reactance ratio versus the outer radius of the DNG shell corresponding to the cases treated earlier are shown in Figs. 4(b), 5(b), and 6(b). It is observed that in all these cases, very good reactance ratios are obtained corresponding to the regions where large power gain values are obtained and also corresponding to the gain peaks. The nature of gain variation with the inner shell radius r_1 is the same as reported in [35] and is not repeated here.

In order to substantiate the gain enhancement further, the radiated power gain is computed by comparing the power radiated by the DNG shell with a reference loop of the same radius as the outer shell. Thus, in this case, the numerator of

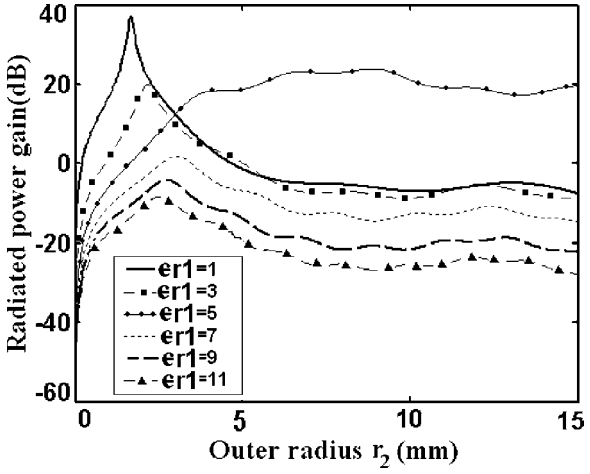

FIG. 8. Radiated power gain of a DNG shell excited by an infinitesimal electric loop compared with a loop antenna with the same radius as the outer radius of the DNG shell, for different values of permittivities in Region 1 and variable outer radius r_2 with inner radius $r_1=30$ μm, $a=30$ μm, $\mu_{r1}=6$, $\varepsilon_{r2}=-1$, $\mu_{r2}=-3$.

(31) is computed in a similar manner as before. For the denominator however, the radiated power is considered for a loop of radius r_2. As such, in this case, the DNG shell is viewed as an antenna excited by an electrically small loop of radius a. The performance of this antenna is compared with respect to a loop of the same radius as the outer radius of the antenna. The radiated power gain in this case is shown in Fig. 8. The expression (5.58) in [23] has been used to compute the power radiated by a loop for the denominator in (31). It is seen that reasonably high power gains are obtained in this case, though the radiated power gain is better in Fig. 7. This is expected as the reference loop radius is greater in Fig. 8, compared to Fig. 7. It is also found that optimum power gain is obtained when the inner radius of the shell r_1 is the same as the radius of the electrically small loop a. The radiated power gain is seen to be best for $\varepsilon_{r1}=1$, $\mu_{r1}=6$, $\varepsilon_{r2}=-1$, $\mu_{r2}=-3$ where a radiated power gain peak occurs at 37.34 dB for $r_2=1.70$ mm. This also corresponds to a thick DNG shell. In addition, uniform gain characteristics are obtained with the media parameters $\varepsilon_{r1}=5$, $\mu_{r1}=6$, $\varepsilon_{r2}=-1$, $\mu_{r2}=-3$, with a gain of more than 20 dB over 5.5 mm$\leqslant r_2 \leqslant$10.38 mm. Also, the gain remains almost uniform for these media parameters up to $r_2=15$ mm. It might be noted that these are the same two sets of parameters for which the best performance was obtained in the case of Fig. 7. Computing the reactance ratio however, in this case is quite involved, as the near fields of the loop must be considered in the denominator of (33) in [35].

In order to study the frequency dependence of the infinitesimal loop with a DNG shell, a Drude model of the DNG medium was used as in (7) of [40]. Both lossless and lossy cases were considered. Since the permittivity and permeability of the DNG shell are different, the corresponding plasma frequencies were fixed at $f_{\varepsilon p}=14.1421$ GHz and $f_{\mu p}=20$ GHz, respectively, to obtain $\varepsilon_{r2}=-1$ and $\mu_{r2}=-3$ at the design frequency of 10 GHz. The collision frequencies for modeling the electric and magnetic losses for the lossy Drude model were set to $\Gamma_\varepsilon=0.0001\omega_{p\varepsilon}$ and Γ_μ

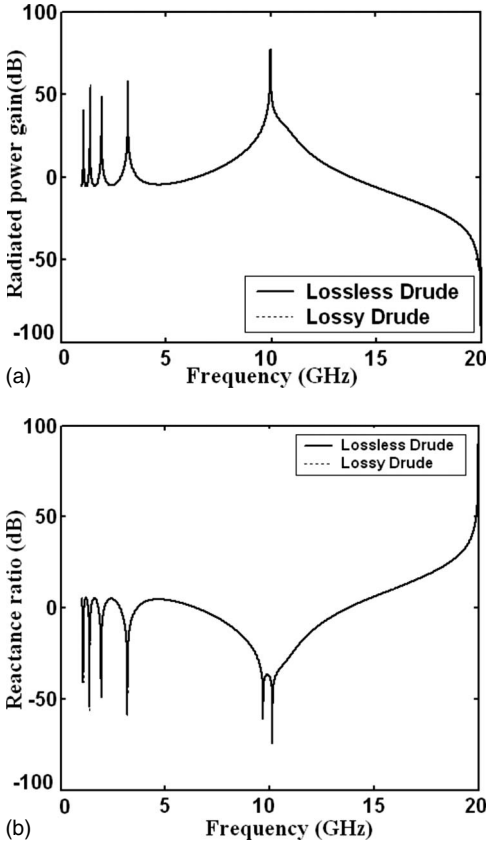

FIG. 9. (a) Radiated power gain and (b) reactance ratio versus frequency for a Drude model DNG shell for the optimized design in case of the electrically small loop with $r_1=100\ \mu$m and $r_2=2.596$ mm, $a=30\ \mu$m, $\varepsilon_{r1}=1$, $\mu_{r1}=6$, $f_{\varepsilon p}=14.1421$ GHz, $f_{\mu p}=20$ GHz corresponding to the gain peak in Fig. 7(a).

$=0.0001\omega_{p\mu}$. The value of the outer shell radius $r_2=2.596$ mm was chosen at the peak of the gain characteristics in Fig. 7(a) for the optimum design parameters $\varepsilon_{r1}=1$, $\mu_{r1}=6$, $\varepsilon_{r2}=-1$, $\mu_{r2}=-3$. It can be seen from Fig. 9(a) that the resonance peak at 10 GHz is quite sharp. This peak can be broadened by varying the inner shell radius r_1, though at a reduced gain level [35]. This is shown in Fig. 10(a), which shows the frequency characteristics using $r_1=400\ \mu$m. It was also found that the gain characteristics for the lossy cases in Figs. 9 and 10 almost coincide with the lossless Drude models and as such are indistinguishable from the lossless cases. The power gains at the design frequency of 10 GHz for the lossless and the lossy cases in Fig. 9(a) are however at 77.48 dB and 74.25 dB, respectively. The corresponding gains for the lossless and lossy cases in Fig. 10(a) are at 43.17 dB and 43.06 dB, respectively.

The Drude model corresponding to Fig. 8 is shown in Fig. 11. The outer radius of the DNG shell is chosen to be $r_2=1.70$ mm for which the gain peak is obtained with the media parameters $\varepsilon_{r1}=1$, $\mu_{r1}=6$, $\varepsilon_{r2}=-1$, $\mu_{r2}=-3$ in Fig. 8. The lossless and the lossy cases in Fig. 11 again almost overlap each other.

The effect of using a MNG shell in place of the DNG medium in region 2 is next investigated. Figure 12(a) shows the comparative performance in gain enhancement using optimized DNG and MNG shells. Two cases are shown for the MNG shell in Fig. 12(a) with parameters $\varepsilon_{r1}=1$, $\mu_{r1}=6$, $\varepsilon_{r2}=1$, $\mu_{r2}=-3$ and $\varepsilon_{r1}=5$, $\mu_{r1}=6$, $\varepsilon_{r2}=1$, $\mu_{r2}=-3$, corresponding to the two optimized designs of the DNG shell.

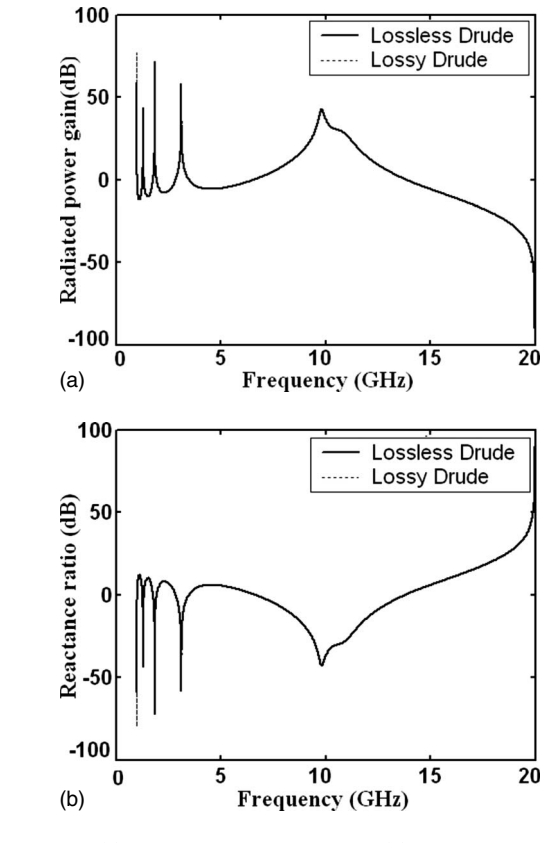

FIG. 10. (a) Radiated power gain and (b) reactance ratio versus frequency for a Drude model DNG shell for the optimized design in case of the electrically small loop with $r_1=400\ \mu$m. The other parameters are the same as in Fig. 9.

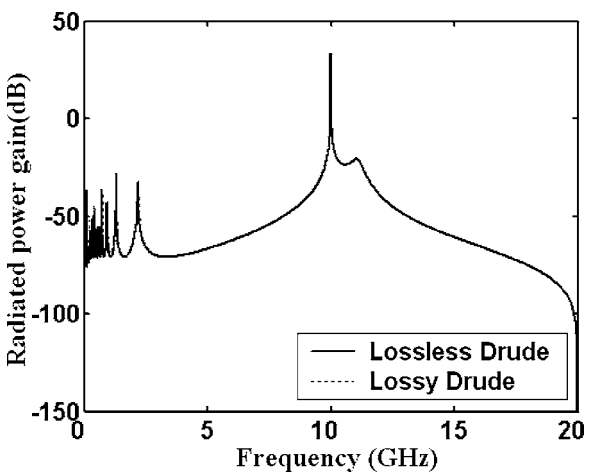

FIG. 11. Radiated power gain versus frequency for a Drude model DNG shell for the optimized design in case of the reference loop of radius r_2 of Fig. 8 with $r_1=30\ \mu$m and $r_2=1.70$ mm, $a=30\ \mu$m, $\varepsilon_{r1}=1$, $\mu_{r1}=6$, $f_{\varepsilon p}=14.1421$ GHz, $f_{\mu p}=20$ GHz, $\Gamma_\varepsilon=0.0001\omega_{p\varepsilon}$, $\Gamma_\mu=0.0001\omega_{p\mu}$ corresponding to the gain peak in Fig. 8.

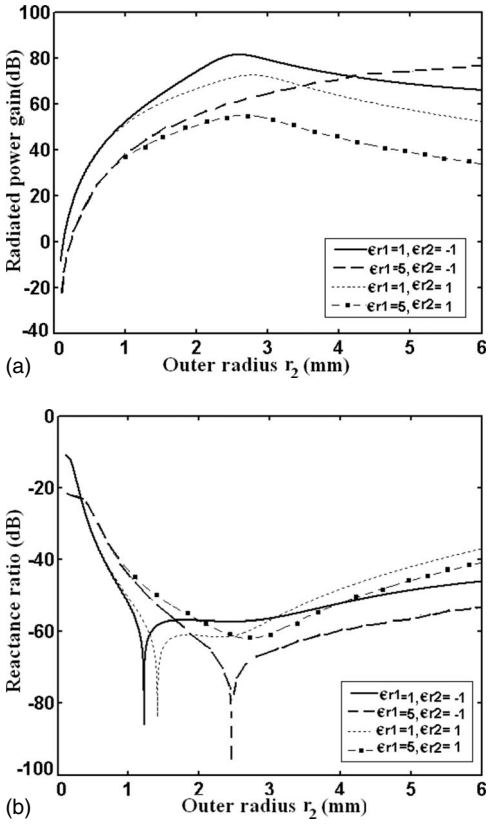

FIG. 12. (a) Radiated power gain and (b) reactance ratio of an infinitesimal electric loop surrounded by optimized DNG and MNG shells and variable outer radius r_2 with inner radius $r_1=100$ μm, $a=30$ μm, $\mu_{r1}=6$, $\mu_{r2}=-3$.

Though moderately high and uniform gain characteristics can be obtained using the former MNG shell, it is seen that the performance of the DNG shell with parameters $\varepsilon_{r1}=1$, $\mu_{r1}=6$, $\varepsilon_{r2}=-1$, $\mu_{r2}=-3$ is improved in comparison with the MNG shell. It might however be noted that realization of a SNG medium is easier than a DNG medium. The trade-off in power gain using a MNG shell with parameters $\varepsilon_{r1}=1$, $\mu_{r1}=6$, $\varepsilon_{r2}=1$, $\mu_{r2}=-3$ is about 8.8 dB less gain compared with the corresponding DNG shell with parameters $\varepsilon_{r1}=1$, $\mu_{r1}=6$, $\varepsilon_{r2}=1$, $\mu_{r2}=-3$ at the respective gain peaks. It should also be noted from Fig. 12(a) that though the best gain characteristics can be obtained using a DNG shell with parameters $\varepsilon_{r1}=5$, $\mu_{r1}=6$, $\varepsilon_{r2}=-1$, $\mu_{r2}=-3$ above $r_2=4.24$ mm, the same is not true of the corresponding MNG shell with parameters $\varepsilon_{r1}=5$, $\mu_{r1}=6$, $\varepsilon_{r2}=1$, $\mu_{r2}=-3$. The reactance ratios for the gain characteristics in Fig. 12(a) is shown in Fig. 12(b). It can be seen that good reactance ratios are obtained corresponding to the radiated power gain for the DNG and the MNG shells. It should also be emphasized that the loop gain is enhanced only when the SNG medium in region 2 is of the MNG type and no power gain can be obtained using an ENG shell in region 2.

Next, the performance of the MNG shell, excited by the electrically small loop is compared with a loop antenna of the same radius as the outer radius r_2 of the MNG shell in Fig. 13. The media parameters have been optimized to obtain the best gain performance. It is seen that reasonably high

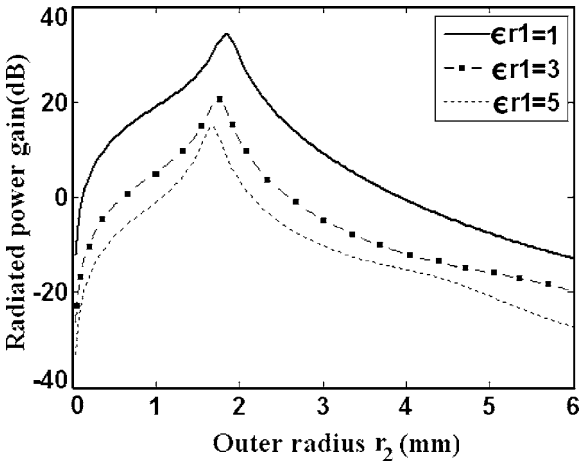

FIG. 13. Radiated power gain of a MNG shell excited by an infinitesimal electric loop compared with a loop antenna with the same radius as the outer radius of the DNG shell, for different values of permittivities in region 1 and variable outer radius r_2 with inner radius $r_1=30$ μm, $a=30$ μm, $\mu_{r1}=4$, $\varepsilon_{r2}=1$, $\mu_{r2}=-2$.

gains are obtained with respect to a loop antenna of the same radius as the outer radius of the MNG shell, though the gain levels in Fig. 12 for the MNG shell are somewhat higher. The peak gain for the case $\varepsilon_{r1}=1$ is found to be at 34.36 dB for $r_2=1.84$ mm in Fig. 13.

All comments above for the gain enhancement of the infinitesimal loop hold true in the case of the electrically small dipole with the permittivity and permeability interchanged. Thus the optimized parameters for the dipole case are $\varepsilon_{r1}=6$, $\mu_{r1}=1$, $\varepsilon_{r2}=-3$, $\mu_{r2}=-1$ for which identical gain characteristics as for the loop are obtained. In fact, performance optimization for the dipole case is relatively easier than for the loop as a dielectric material with a permittivity of 6 can be used in region 1 in the dipole case. For the loop, however, a material with $\mu_{r1}=6$ is required in region 1 which should be obtained using ferromagnetic media. In addition, gain enhancement for the electrically small dipole can be accomplished using an ENG shell with media parameters $\varepsilon_{r1}=6$, $\mu_{r1}=1$, $\varepsilon_{r2}=-3$, $\mu_{r2}=1$ similar to the power gain obtained for the loop with the MNG shell.

B. Air-DPS-free space

In this section, the effect of using a DPS shell in region 2 is studied. The particular advantage of the DPS shell is its ease of manufacture compared to a metamaterial shell. In addition, compared to DNG media which possess dispersive behavior with frequency, DPS materials are nondispersive. It is shown here that considerable high gains are also possible for an electrically small antenna using a DPS shell of the same size as a metamaterial shell. To the best knowledge of the authors, gain enhancement of electrically small antennas using DPS shells has not been reported. As in the case of the metamaterial shell of Sec. IV A, verification using HFSS was not possible due to the lack of availability of the high computational resource. As such, fabrication and measurements with the DPS shell could not be done as it would require precise design and simulation of the feed dimensions to the

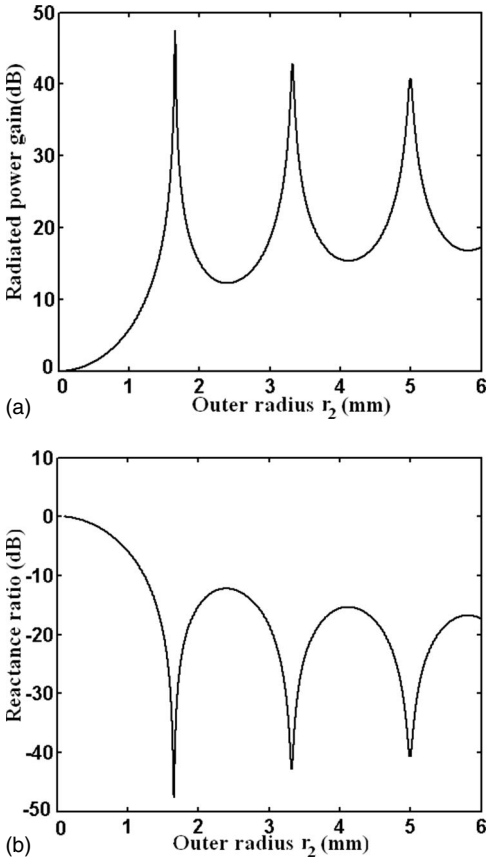

FIG. 14. (a) Radiated power gain and (b) reactance ratio of an infinitesimal electric loop surrounded by a DPS shell and variable outer radius r_2 with inner radius $r_1=100$ μm, $a=30$ μm, $\varepsilon_{r1}=1$, $\mu_{r1}=1$, $\varepsilon_{r2}=80$, $\mu_{r2}=1$.

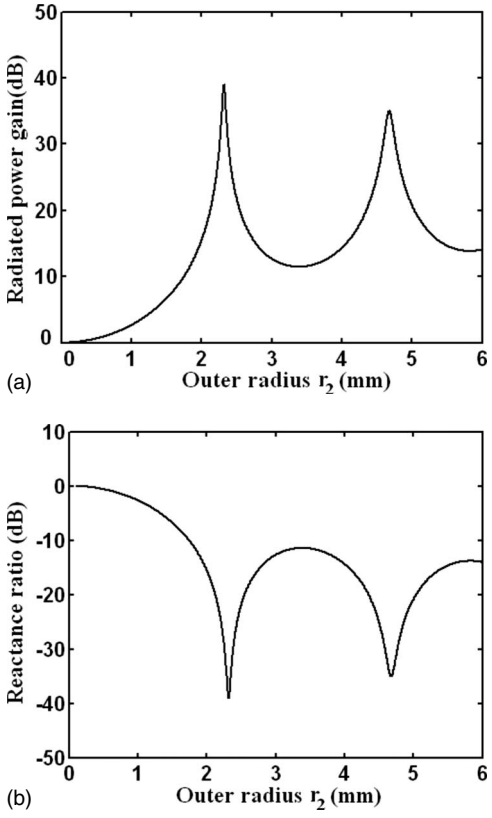

FIG. 15. (a) Radiated power gain and (b) reactance ratio of an infinitesimal electric loop surrounded by a DPS shell and variable outer radius r_2 with inner radius $r_1=100$ μm, $a=30$ μm, $\varepsilon_{r1}=1$, $\mu_{r1}=1$, $\varepsilon_{r2}=40$, $\mu_{r2}=1$.

electrically small loop [40]. The reliability of the following results is based on the fact that corresponding results for the metamaterial shell using the same methodology were verified by HFSS in [40].

The same antenna dimensions and inner shell radius as for the metamaterial shell in Fig. 7 is used. In the first case, the parameters of region 1 and region 2 are chosen as $\varepsilon_{r1}=1$, $\mu_{r1}=1$, $\varepsilon_{r2}=80$, $\mu_{r2}=1$. The power gain is shown in Fig. 14(a). It can be observed that several distinct peaks in the power gain characteristics appear as the outer radius of the DNG shell is varied. The first gain peak is at the highest level of 47.60 dB at a outer shell radius of $r_2=1.655$ mm. The peaks slowly decrease in amplitude from the first to the third gain peak which is at 40.36 dB for $r_2=5$ mm. This is unlike the gain characteristics obtained using the metamaterial shell over the same range of variation of the outer shell radius. As seen in Section IV A, a metamaterial shell can be designed to achieve large and uniform gain characteristics with suitable choice of media parameters in regions 1 and 2. It can be seen from Fig. 14(a) that, compared to a metamaterial shell, high power gains for the electrically small loop at multiple values of outer shell radius are obtained with a DPS shell of the same dimensions as the metamaterial shell. The peak gains in Fig. 14(a) with the DPS shell, though quite high, are lower than in Fig. 7(a) with the metamaterial shell. However, it was verified that the peak gains in Fig. 14(a) could be increased by using a dielectric with a higher permittivity in region 2. The resonance characteristics with r_2 of course becomes sharper with an increase in permittivity of the DPS shell due to an enhanced Q factor of the antenna. Figures 15(a) and 16(a) show the gain characteristics with the permittivity of the DPS shell as 40 and 20, respectively. As expected, a broader resonance behavior is observed as the permittivity of the DPS shell decreases. The peak gains for the first resonances in Fig. 14(a) and Fig. 15(a) are 47.60 dB and 39.05 dB, respectively, while it is 30.77 dB for the resonance in Fig. 16(a). Thus, the peak gains decrease as ε_{r2} decreases, with greater design tolerance. It can also be seen from Fig. 14(a), 15(a), and 16(a) that an increase in permittivity of the DPS shell increases the number of gain peaks within the same range of values of r_2. As the permittivity of region 2 increases, the resonance characteristics versus r_2 shifts to the left, as is expected, with corresponding reduction in antenna size. However, it might be noted that the size of the resonator with the DPS shell is exactly the same as the metamaterial shell surrounding the loop.

Figures 14(b), 15(b), and 16(b) show the corresponding reactance ratios versus the outer shell radius using the DPS shell for $\varepsilon_{r2}=80$, 40, and 20, respectively. It is seen that the dips in the reactance ratio with varying r_2 occur at exactly the same values of r_2 corresponding to the power peaks in Fig. 14(a), Fig. 15(a), and Fig. 16(a). Thus, though the gain resonances are narrower with the DPS shell, excellent match-

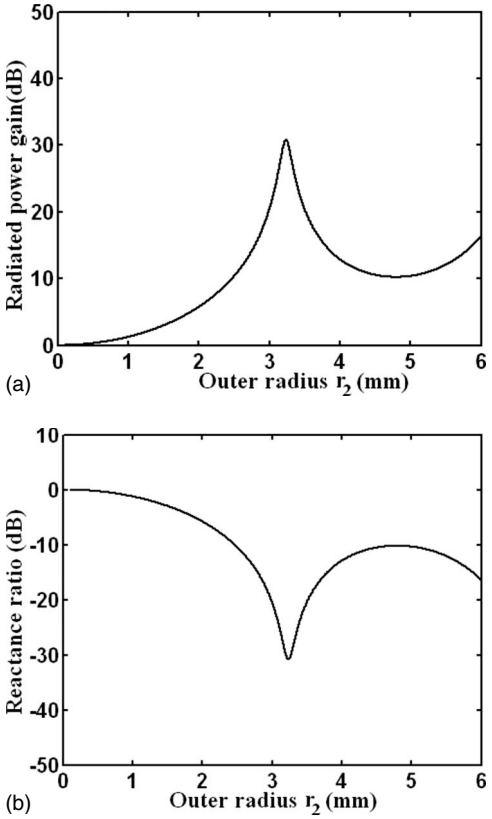

FIG. 16. (a) Radiated power gain and (b) reactance ratio of an infinitesimal electric loop surrounded by a DPS shell and variable outer radius r_2 with inner radius $r_1=100$ μm, $a=30$ μm, $\varepsilon_{r1}=1$, $\mu_{r1}=1$, $\varepsilon_{r2}=20$, $\mu_{r2}=1$.

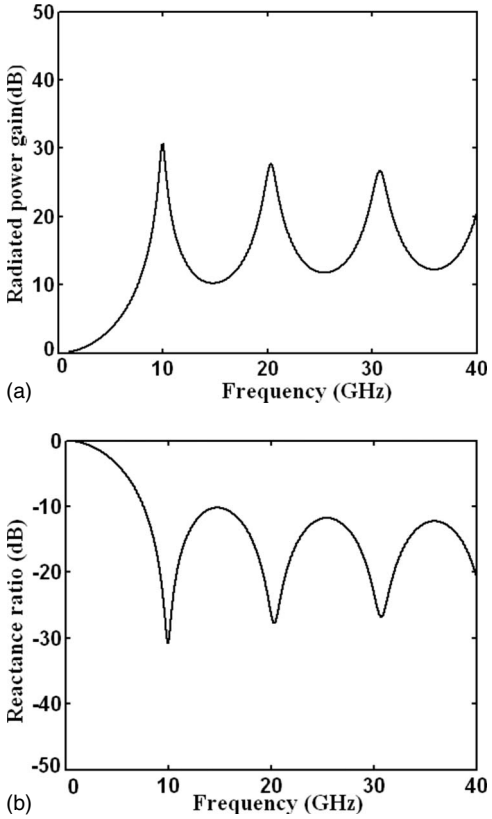

FIG. 17. (a) Radiated power gain and (b) reactance ratio versus frequency of an infinitesimal electric loop surrounded by a DPS shell with $r_1=100$ μm, $r_2=3.2380$ mm, $a=30$ μm, $\varepsilon_{r1}=1$, $\mu_{r1}=1$, $\varepsilon_{r2}=20$, and $\mu_{r2}=1$, corresponding to the gain peak in Fig. 16(a).

ing conditions exist at the power gain resonances. The performance of the DPS shell in enhancing the power gain of the electrically small loop is summarized in Table I.

The power gain versus frequency with $\varepsilon_{r2}=20$ for the DPS shell is shown in Fig. 17(a). An optimum outer shell radius of $r_2=3.2380$ mm is chosen corresponding to the gain peak in Fig. 16(a). In order to investigate the resonant frequencies for the DPS shell where the power gains are maximum, it is necessary to view the DPS shell as a two-layer DRA, with the electrical loop as the excitation source. The inner medium of the two-layer DRA is free space while the second layer is of permittivity 20. The full-wave Green's function of a N-layer DRA has been reported in [54]. From the analysis presented in [54], the source free resonant frequencies of a multilayer DRA can be obtained from the zeroes of the determinant corresponding to the matrix equation for determination of the unknowns of the homogeneous Green's function. The source free resonances for both the TM_{nmp} and the TE_{nmp} modes of the N-layer DRA were thus obtained. The first and second subscripts in the mode designation refer to the order of the spherical Bessel function (Schelkunoff type) and the azimuthal variation of the field, respectively. The third subscript refer to the ordered zeroes of the spherical Bessel function. It can also be noted that the eigenvalues "m" correspond to degenerate modes and can be identified from the field distribution of the mode. It was found that for a two-layer DRA of the same layer thicknesses and layer permittivities as of the DPS shell in Fig. 17, the

TABLE I. Performance of the electrically small circular loop surrounded by DPS shell for different values of relative permittivity ε_{r2} with $r_1=100$ μm, $a=30$ μm, $\varepsilon_{r1}=1$, $\mu_{r1}=1$, and $\mu_{r2}=1$.

Relative permittivity ε_{r2}	Outer shell radius r_2 (mm) corresponding to the first power gain peak	Percentage 3 dB bandwidth at the			Maximum radiated power gain (dB) at the		
		First peak	Second peak	Third peak	First peak	Second peak	Third peak
20	3.2380	4.790			30.77		
40	2.3225	2.029	2.537		39.05	35.03	
80	1.6550	0.779	1.180	1.2564	47.60	42.65	40.36

source-free resonances for the TE_{1m1}, TE_{1m2}, and TE_{1m3} modes are at 9.99 GHz, 20.34 GHz, and 30.76 GHz, respectively. These exactly match with the power gain resonances of the electrically small loop surrounded by the DPS shell in Fig. 17(a).

The gain peaks after the first resonance at 10 GHz are of gradually diminishing amplitudes with the third gain peak at about 26.75 dB. The corresponding reactance ratio versus frequency is shown in Fig. 17(b). Excellent matching characteristics are seen corresponding to the gain peaks in Fig. 17(a). It can also be observed from Fig. 17 that an infinitesimal loop surrounded by a DPS shell behaves as a multiband antenna.

It might also be noted that an identical power gain using a DPS shell can be obtained for an electrically small dipole by interchanging the permittivity and permeability of the DPS shell. Hence, in case of the dipole, the gain resonances can be obtained by using a ferromagnetic material with nonunity permeability for the DPS shell. The power gain peaks versus frequency in this case occur exactly at the same frequencies as for the electrically small loop. However, these frequencies with the changed material parameters for the shell correspond to the source-free TM_{nmp} resonances of the two-layer DRA. Though a very detailed study with intuitive insights as to the interaction of the antenna and the metamaterial shell have been originally outlined in [35–40,42], the authors would like to state that the proposition in [42] that a DPS shell does not enhance the gain of an electrically small antenna is different from our current conclusion.

It was also found that power gain, when compared to a loop of the same radius as the outer radius of the DPS shell, could not be obtained with the DPS shell.

V. CONCLUSIONS

The radiated power gain of an infinitesimal loop using a metamaterial and a DPS shell was investigated. It was observed that a metamaterial shell can be used to enhance the gain of the electrically small loop. This is due to the fact that, similar to the small dipole, the reactive part of the radiated power for the infinitesimal loop changes in sign in the DNG medium compared to that in a DPS medium. As the electrical loop can be considered equivalent to an orthogonally oriented slot antenna, efficient slot antennas can be designed based on this phenomenon.

A parametric optimization was done to study the effect of the media parameters on the gain characteristics. It was observed that for the loop antenna surrounded by the DNG shell, with the inner medium as free space, the power gain can be tuned with variation in the permeability of the DNG shell while varying the permittivity of the shell has no effect. However, the resonance characteristics using free space as the inner medium are too sharp for practical implementation. The variation in power gain versus the outer shell radius can be made more uniform by a proper choice of permeability of the inner medium. Optimum power gain characteristics were obtained using a permeability of 6 for the inner medium. In addition, with a material of nonunity permeability filling the inner region, the permittivity of the DNG shell has a significant impact on the gain profile, unlike the case where the inner medium is free space. High and stable radiated power gain was obtained over a wide range of DNG shell thickness, by a suitable choice of material parameters. This considerably eases the design of the metamaterial shell. Very good reactance ratios were obtained corresponding to the entire uniform gain region in all cases. This ensures excellent matching conditions for the loop surrounded by the DNG shell. In addition, good power gain characteristics were obtained when the radiated power from the DNG shell excited by an electrically small loop was compared with the power radiated by a loop of the same radius as the outer radius of the DNG shell. The power gain obtained when the radiated power of the electrically small loop in the presence of the DNG shell was compared with the power radiated by the electrically small loop in the absence of the DNG shell were however better, as expected.

A Drude model for the DNG shell was used to study the frequency dependence of the antenna surrounded by the metamaterial shell. It was also seen that an MNG shell can be used to enhance the gain of the infinitesimal loop and offer uniform gain characteristics versus the outer shell radius. Though the power gain characteristics obtained using a DNG shell are improved in comparison to that with the MNG shell, it might be noted that SNG media are easier to realize than DNG materials. It is also possible to use the MNG shell to significantly increase the radiated power gain of the shell excited by an electrically small loop with respect to a loop of the same radius as the outer radius of the MNG shell.

For an infinitesimal dipole surrounded by a DNG or a SNG shell, similar power gain and reactance ratio characteristics are obtained as for the electrically small loop with the media permittivities and permeabilities interchanged. A particular advantage in this case is that the optimized permittivity of the inner medium should be 6 which is much easier to realize compared to a corresponding permeability of 6 for the inner medium in the loop antenna case. Also, the SNG shell used for gain enhancement of the dipole should be of the ENG type.

The gain enhancement of the infinitesimal loop using a DPS shell was next addressed. The dimensions of the DPS shell were maintained the same as the metamaterial shell. Distinct power gain peaks versus the outer shell radius were observed in this case. This can be contrasted to the gradual variation in gain over a much larger range of outer shell radius obtained using the metamaterial shell. The gain profile of the infinitesimal loop surrounded by the DPS shell can be explained by considering the loop as the excitation source to the two-layer DRA formed by the inner medium and the DPS shell. The radiated power gain versus frequency for the antenna with the DPS shell shows multiple peaks corresponding to the source free TE resonant frequencies of the two-layer DRA. A similar power gain profile with a DPS shell can be obtained for the electrically small dipole by interchanging the shell permittivity and permeability for the case of the infinitesimal loop.

[1] V. G. Veselago, Supercond., Phys. Chem. Technol. **10**, 509 (1968) [Usp. Fiz. Nauk **92**, 517 (1967)].
[2] J. B. Pendry, A. J. Holden, D. J. Robbins, and W. J. Stewart, IEEE Trans. Microwave Theory Tech. **47**, 2075 (1999).
[3] D. R. Smith, W. J. Padilla, D. C. Vier, S. C. Nemat-Nasser, and S. Schultz, Phys. Rev. Lett. **84**, 4184 (2000).
[4] R. W. Ziolkowski and E. Heyman, Phys. Rev. E **64**, 056625 (2001).
[5] R. W. Ziokowski, IEEE Trans. Antennas Propag. **51**, 1516 (2003).
[6] N. Engheta, IEEE Antennas Wireless Propag. Lett. **1**, 10 (2002).
[7] Y. Li, L. Ran, H. Chen, J. Huangfu, X. Zhang, K. Chen, T. M. Grzegorczyk, and J. A. Kong, IEEE Trans. Microwave Theory Tech. **53**, 1522 (2005).
[8] D. M. Grimes and C. A. Grimes, Microwave Opt. Technol. Lett. **28**, 172 (2001).
[9] R. E. Collin, J. Electromagn. Waves Appl. **12**, 1369 (1998).
[10] L. J. Chu, J. Appl. Phys. **19**, 1163 (1948).
[11] R. E. Collin and S. Rothschild, IEEE Trans. Antennas Propag. **12**, 23 (1964).
[12] H. A. Wheeler, IEEE Trans. Antennas Propag. **23**, 462 (1975).
[13] H. A. Wheeler, Proc. IRE **47**, 1325 (1959).
[14] R. C. Hansen, Proc. IEEE **69**, 170 (1981).
[15] J. S. McLean, IEEE Trans. Antennas Propag. **44**, 672 (1996).
[16] A. D. Yaghjian and S. R. Best, IEEE Trans. Antennas Propag. **53**, 1298 (2005).
[17] R. L. Fante, IEEE Trans. Antennas Propag. **17**, 151 (1969).
[18] G. S. Smith, IEEE Trans. Antennas Propag. **40**, 369 (1977).
[19] S. R. Best, IEEE Trans. Antennas Propag. **52**, 953 (2004).
[20] S. R. Best, IEEE Antennas Propag. Mag. **46**, 9 (2004).
[21] S. R. Best, IEEE Trans. Antennas Propag. **53**, 502 (2005).
[22] S. R. Best, IEEE Trans. Antennas Propag. **53**, 1047 (2005).
[23] C. A. Balanis, *Antenna Theory*, 3rd ed. (Wiley, New York, 2005).
[24] R. F. Harrington, *Time Harmonic Electromagnetic Fields* (McGraw-Hill, New York, 1961).
[25] G. Skahill, R. M. Rudish, and J. Piero, *Proceedings of the Antenna Applications Symposium, Allerton Park, Monticello, IL, 1998* (unpublished).
[26] E. E. Altshuler, IEEE Trans. Antennas Propag. **50**, 297 (2002).
[27] L. Fante, IEEE Trans. Antennas Propag. **40**, 1586 (1992).
[28] E. E. Altshuler, IEEE Trans. Antennas Propag. **50**, 297 (2002).
[29] K. M. Chen and C. C. Lin, Proc. IEEE **56**, 1595 (1968).
[30] M. G. Andreasen, IRE Trans. Antennas Propag. **5**, 337 (1957).
[31] H. R. Raemer, IRE Trans. Antennas Propag. **10**, 69 (1962).
[32] R. V. Row, IEEE Trans. Antennas Propag. **12**, 646 (1964).
[33] S. A. Tretyakov, S. I. Maslovski, A. A. Sochaya, and C. R. Simovski, IEEE Trans. Antennas Propag. **53**, 965 (2005).
[34] H. B. Keller and J. B. Keller, J. Appl. Phys. **20**, 393 (1949).
[35] R. W. Ziolkowski and A. D. Kipple, IEEE Trans. Antennas Propag. **51**, 2626 (2003).
[36] R. W. Ziolkowski and A. D. Kipple, Phys. Rev. E **72**, 036602 (2005).
[37] R. W. Ziolkowski, *IEEE International Workshop on Antenna Technology: Small Antennas and Novel Metamaterials, Singapore, 2005*, (IEEE, Piscataway, 2005), pp. 7–10.
[38] A. Erentok and R. W. Ziolkowski,Digest of the IEEE AP-S International Symposium, Washington, DC, 2005, (IEEE, Piscataway, 2005) pp. 22–25.
[39] A. Erentok and R. W. Ziolkowski, *IEEE International Workshop on Antenna Technology: Small Antennas and Novel Metamaterials*, (IEEE, Piscataway, 2006), pp. 400–403.
[40] R. W. Ziolkowski and A. Erentok, IEEE Trans. Antennas Propag. **54**, 2113 (2006).
[41] P. D. Imhof, R. W. Ziolkowski, and J. R. Mosig, *Digest of the IEEE AP-S International Symposium, Albuquerque, NM, 2006*, (IEEE, Piscataway, 2006), pp. 1927–1930.
[42] A. Erentok and R. W. Ziolkowski, IEEE Trans. Antennas Propag. **55**, 731 (2007).
[43] R. W. Ziolkowski, *Digest of the IEEE AP-S International Symposium, Honolulu, Hawaii, 2007*, (IEEE, Piscataway, 2007), pp. 3313–3315.
[44] A. Alu and N. Engheta, IEEE Trans. Antennas Propag. **55**, 3027 (2007).
[45] R. W. Ziolkowski and A. Erentok, IET Proc. Microwaves, Antennas Propag. **1**, 116 (2007).
[46] S. Arslanagic, R. W. Ziolkowski, and O. Breinbjerg, *International Workshop on Antenna Technology: Small and Smart Antennas Metamaterials and Applications, Cambridge, UK, 2007*, (IEEE, Piscataway, 2007), pp. 376–379.
[47] S. Arslanagic, R. W. Ziolkowski, and O. Breinbjerg, *Digest of the IEEE AP-S International Symposium, Albuquerque, NM, 2006*, (IEEE, Piscataway, 2006) pp. 676–679.
[48] A. Erentok and R. W. Ziolkowski, Microwave Opt. Technol. Lett. **49**, 1287 (2007).
[49] A. Erentok and R. W. Ziolkowski, Microwave Opt. Technol. Lett. **49**, 1669 (2007).
[50] A. Erentok and R. W. Ziolkowski, *International Workshop on Antenna Technology: Small and Smart Antennas Metamaterials and Applications, Cambridge, UK, 2007*, (IEEE, Piscataway, 2007), pp. 19–22.
[51] A. Erentok and R. W. Ziolkowski, *Digest of the IEEE AP-S International Symposium, Honolulu, Hawaii, 2007*, (IEEE, Piscataway, 2007), pp. 1877–1880.
[52] A. Erentok and R. W. Ziolkowski, *Digest of the IEEE AP-S International Symposium, Honolulu, Hawaii, 2007*, (IEEE, Piscataway, 2007) pp. 1861–1864.
[53] M. Abramowitz and I. A. Stegun, *Handbook of Mathematical Functions* (Dover, New York, 1974), Chap. 10.
[54] A. B. Kakade and B. Ghosh, IEEE Trans. Antennas Propagat (to be published).